



## Deposition Environment Interpretation of Lemat Formation in the West Tanjung Jabung, Jambi Province

Sapto Kis Daryono\*<sup>1</sup>, Afrilita<sup>1</sup>, Idarwati<sup>2</sup>

<sup>1</sup> Faculty of Mineral Technology, Universitas Pembangunan Nasional, Yogyakarta, Indonesia

<sup>2</sup> Faculty of Engineering, Universitas Sriwijaya, Palembang, Indonesia

\*E-mail: [kisdaryono@upnyk.ac.id](mailto:kisdaryono@upnyk.ac.id)

### Article info

Received:

Feb 13, 2024

Revised:

Feb 18, 2024

Accepted:

Jun 22, 2024

Published:

Mar 31, 2024

### Keywords:

geology,  
architectural  
element, deposit  
environment,  
facies analysis

### Abstract

The study of facies analysis and interpretation of the depositional environment of the Lemat Formation located on Bukit Tigapuluh aimed to clarify the problems found in Paleogene sediments in the South Sumatra Basin. The results of research on facies analysis and interpretation of the depositional environment of the Lemat Formation will provide an explanation and description of the history of the formation and stratigraphic evolution of Paleogene-aged sedimentary rocks in the South Sumatra Basin as reflected in their lithological and facies characteristics. A detailed analysis of fluvial facies was carried out in the West Tanjung Jabung area, Jambi Province. A stratigraphic cross-section was prepared with an accumulated thickness of  $\pm 25$  m. The stratigraphic section included two rock deposits, namely sandstone-quartz deposits and conglomerate deposits. Analysis of lithofacies and architectural elements of the study area indicated a fluvial depositional environment. The resulting architectural elements consisted of six associations: channel (CH), scour hollows (HO), gravel bedform (GB), sediment gravity flows (SG), sandy bedform (SB), and floodplain fines (FF). The dominance of sedimentary material, which tends to be coarse, and the many facies associations GB, SG, and SB indicated many river bars and were characteristic of braided rivers. The obtained interpretation of the depositional environment was Conglomerate deposits in the Alluvial Fans System with Gravity Flow River environment or gravel bed braided river, and sandstone-gravel deposits in the shallow environment or gravel bed braided river.

## 1. Introduction

The research area was geographically in West Tanjung Jabung Regency, Jambi Province. The research area was part of the South Sumatra Basin, especially the Jambi sub-basin, a basin formed in the back-arc basin (see Figure 1). The stratigraphy of the South Sumatra Basin consists of one giant cycle of sedimentation, starting from the transgression phase at the beginning of the cycle and ending with the regression phase at the end of the cycle [1]. The Lemat Formation has an essential role in the petroleum system in the South Sumatra Basin. The geology and stratigraphy of the South Sumatra Basin have been reported in many studies [2],[3],[4],[5]. The basin's stratigraphy and structural evolution have been a subject of interest, with findings suggesting a shared history with the Central Sumatra Basin [6],[7].

Additionally, research has highlighted the tectonic activities that shaped the basin during the Tertiary Period, emphasizing the role of tectonic forces in its formation [8],[9]. However, the problem of stratigraphic evolution still needs to be solved because land deposits dominate the Paleogene rocks in the basin. Knowing each lithological unit's age, distribution, and source is difficult.

The South Sumatra Basin is located onshore in Sumatra, Indonesia. The research area was part of the northern part of the Jambi Sub-Basin. The Jambi Sub-Basin is bounded to the north by the Tigapuluh Mountains, to the south by the Twelve Mountains, to the west by the Barisan Mountains, and to the east by the Sunda Shelf. The lithostratigraphic naming of the South Sumatra Basin differs for each researcher, especially for Paleogene deposits. Differences in lithostratigraphic nomenclature relate to the description of Paleogene pre-rift, syn-rift, and post-rift deposits. The stratigraphy of the South

Sumatra basin according to [10], as seen as Figure 1, is in a stratigraphic sequence from old to young, successively composed of Pre-tertiary rocks, the Kikim Formation, the Lahat Group (Lemat Formation and Benakat Formation), the Telisa Group, the Tanjung Baru Formation, Talangakar Formation, Gumai Formation, and Baturaja Formation), Palembang Group (Air Benakat Formation, Muara Enim Formation, Kasai Formation), and Quaternary Deposits. The Lemat Formation is interpreted as an Early Oligocene syn-rift sequence deposited in a paleo-low or graben [11]; this unit is not in the paleo-high (especially horst-type structures).

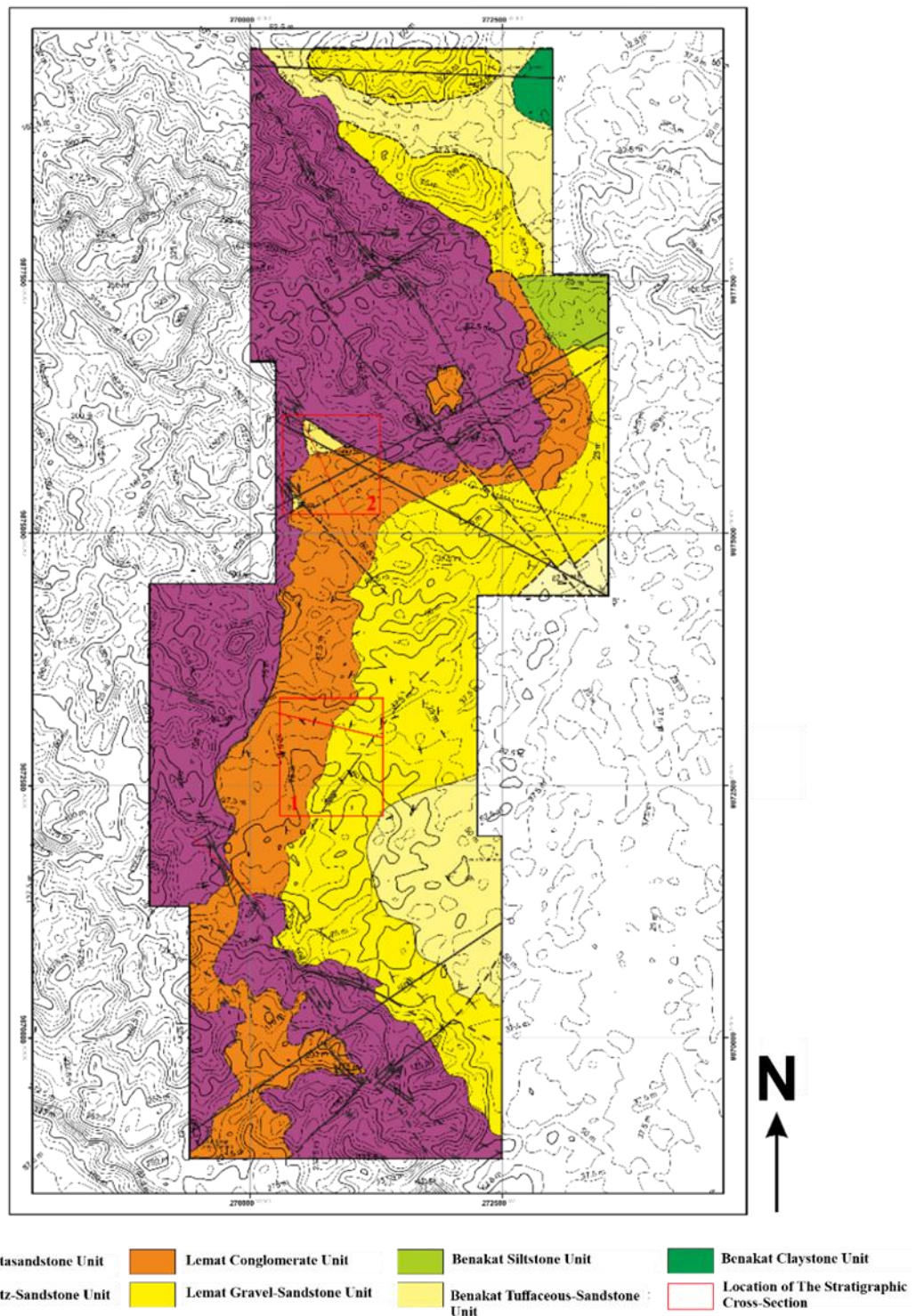


**Figure 1.** Geological map of Bukit Tigapuluh National Park, West Tanjung Jabung, Jambi Province.

**Table 1.** Lithofacies found in each deposit

<b>Facies</b>	<b>Conglomerate deposit</b>	<b>Sandstone-gravel deposit</b>	<b>Sandstone-Quartz deposit</b>
Gmg (matrix-supported gravel)	v	-	v
Gmm (matrix-supported gravel)	v	-	-
Gcm (clast-supported, massive gravel)	v	v	-
Gh (clast-supported, horizontally stratigraphic gravel)	v	-	-
Gp (planar- cross-bedded gravel)	v	v	-
St (trough-cross-bedded sand)	-	v	v
Sh (horizontally bedded sand)	v	v	v
SI (low-angle cross-bedded sand_	-	v	v
Ss (scour-fill sand)	-	v	v
Sm (massive sand)	v	v	v
Fsm (laminated sandstone and mudstone)	-	v	v
FI (laminated mudstone to siltstone)	-	v	-
C (coal, carbonaceous mud)	-	v	-

The Lemat Formation consists of interbedded non-marine sandstone, siltstone, and shale, which turns into shale towards deeper basins, and in some areas, this formation contains tuffaceous material. The island of Sumatra is interpreted to have been formed by the colliding and suturing of microcontinents at the end of the Pre-Tertiary [1], [2], [12]. Four main patterns of geological structure in the research area were the Sunda Pattern trending North-South, the Lematang Pattern trending West-Northwest-East-Southeast (WNW)-(ESE), the Jambi Pattern trending Northeast-Southwest (NE-SW), and the Sumatra pattern tends Southeast - Northwest (SE - NW) [2].

Studies on facies analysis and interpretation of the depositional environment of the Lemat Formation located on Bukit Tigapuluh can clarify the problems found in Paleogene sediments in the South Sumatra Basin. This research was related to the stratigraphy (based on sedimentological analysis) of Paleogene sedimentary rocks, the Jambi Subbasin, mainly from surface samples. Based on that, researchers are interested in examining the depositional architectural elements of the Lemat Formation to understand the geological processes that occur in rocks, which can be identified from the description of the lithofacies of the Lemat Formation. The results of this research will explain and describe the depositional environmental conditions that occurred during the formation of the Lemat Formation as reflected in its lithological and facies characteristics.

## 2. Methodology

Based on the previous study [13], the approach was divided and named based on differences in grain size, relationships between grains, and sedimentary structures specific to sedimentary rocks deposited in fluvial environments. Determination of the Lemat Formation facies referred to the Miall classification [13], [14], [15], using primary data obtained from field mapping results. Field data was in the form of vertical profiles showing the facies aspects of each representative observation location, namely those with specific lithological characteristics and good outcrops. The determination of facies started with lithofacies grouping based on differences in grain size and relationships between grains and sedimentary structure, and then the facies associations were determined. Based on the facies associations found, interpretation results were obtained regarding the depositional environment, geometry of architectural elements, and depositional mechanisms of the Lemat Formation.

## 3. Results and discussion

Based on the stratigraphic cross-section, two rock deposits were obtained: conglomerate and gravelly sandstone. A stratigraphic cross-section was amalgamated based on the profiles at the observation location. The stratigraphic section was in the West Tanjung Jabung area with a stratigraphic section thickness ranging from  $\pm 25$  m. The following facies were determined based on the physical characteristics of the rock.



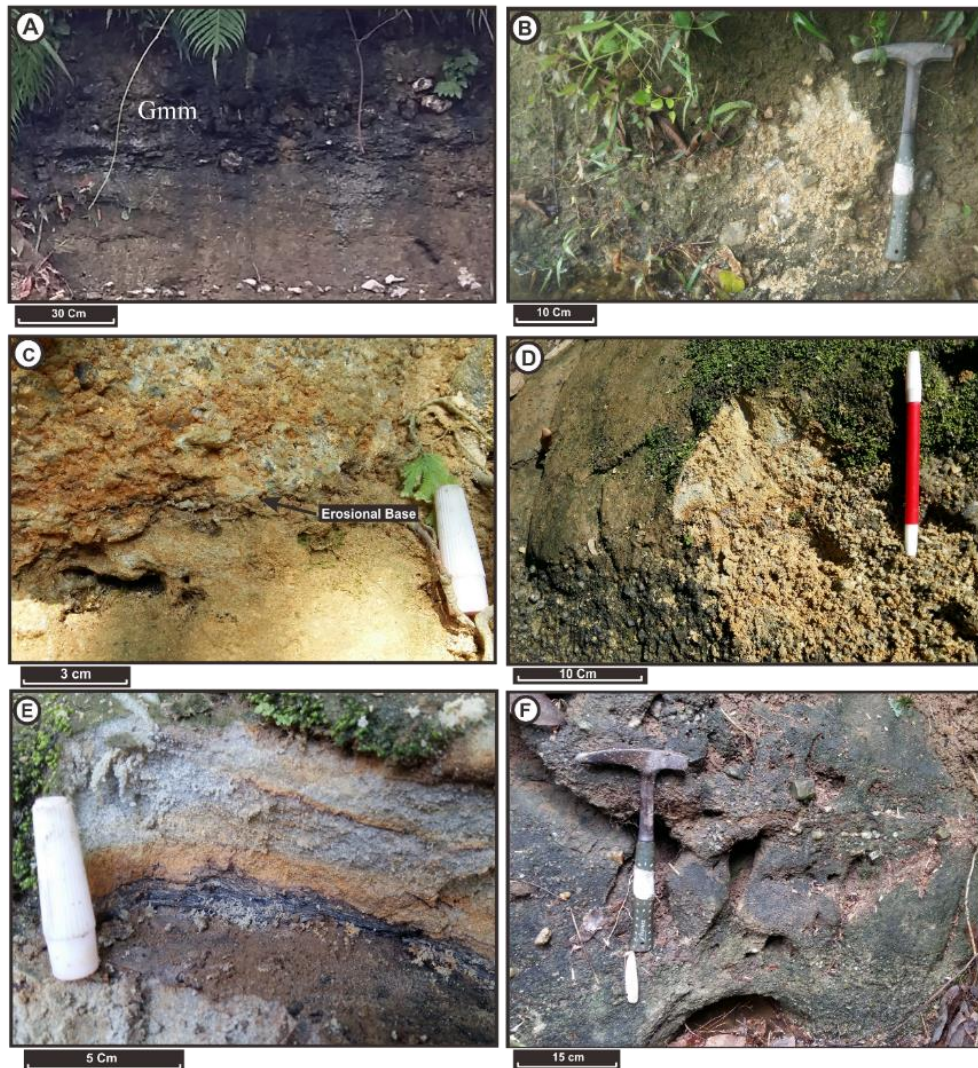


**Figure 2.** (a) The upper part consists of a poorly sorted, sub-rounded-angular conglomerate (facies gmm), and the lower part shows the presence of imbricated clasts (facies Gh). (b) Conglomerate (facies Gmm). (c) Upper conglomerate (Gcm facies) and lower sandstone (Sm facies) separated by an erosional plane. (d) Sandstone (Sm facies) and the lower part is conglomerate with supported clasts (Gcm facies). (e) sandstone with parallel lamination and flaser sandstone structures (facies Sh). (f) Interbedded conglomerate (facies Gmg) and medium-sized sandstone (facies Sm and Ss).

### 3.2. *Litofacies sediment analysis*

There were 13 lithofacies in conglomerate, sandstone-gravel, and sandstone-quartz deposits (see Table 1). Most of it was dominated by sandstone to conglomerate. Mudstone-dominated facies were less typical or even absent in individual outcrops.

#### *Conglomerate deposit*

In this deposit, seven lithofacies were found in the conglomerate deposit [13]. The lithofacies Gcm, Gmg, Gp, Gh, Gmm, Gci, Sm, and Sh were developed in these conglomerate deposits. The Gcm, Gmm, Gci, Gp, and Gh facies developed on polymeric conglomerate lithology and gravelly sandstone. The sedimentary structures were layered, planar criss-crossed, and massive (see Figure 2a). The Gcm facies were interpreted to have been deposited in a high-energy debris flow rich in clastics. The Gmm facies were interpreted as resulting from a low-energy debris flow with a high viscosity level. The Gp facies were interpreted as the result of a migratory channel-filling process (Figure 2c). The Gh facies were interpreted as lag deposits and longitudinal bedforms from deposition in the river system. The Sm and Sh facies developed on medium-sized sandstone – gravelly lithology. The sedimentary structures were massive and ripple cross-lamination (Figure 2e).



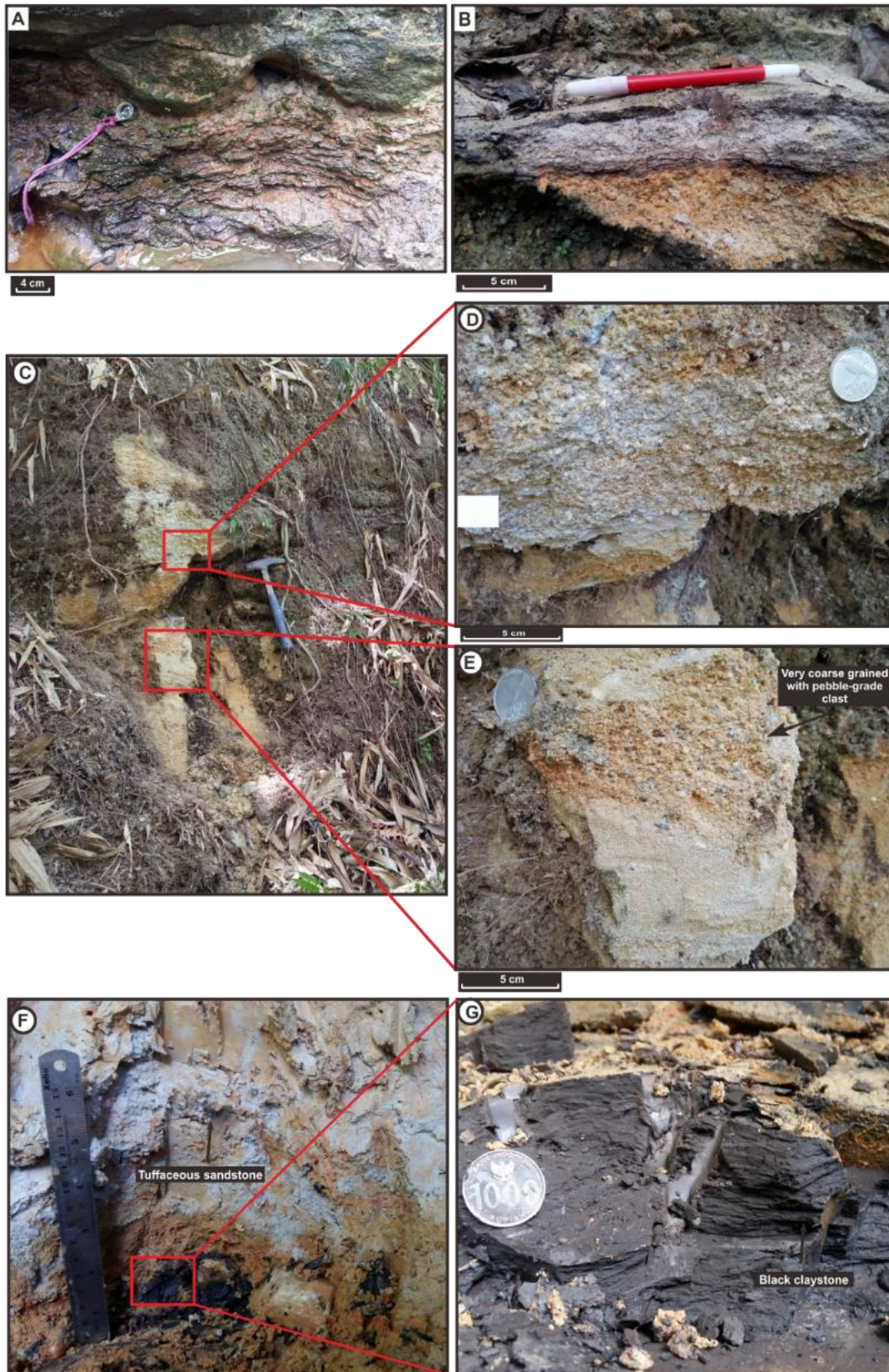


**Figure 3.** (a) Siltstone has a groove cast structure at the bottom (F1), and the top part is massive gravelly sandstone (Sh). (b) Lower massive tuffaceous sandstone (Sm facies) and upper layered sandstone (Sh facies). (c) Conglomerate outcrop with sandstone. (d) close-up of the upper conglomerate with cross-bedding structure (facies Gcm). (e) close-up of lower conglomerate with cross-bedding structure (Facies Gp, Sp, Sh). (f) Sandy tuff (Fsm facies). (g) Carboniferous mudstone (facies C).

### *Sandstone-gravel deposit*

Eight lithofacies types were found in the sandstone-gravel deposits based on the division of lithofacies [13]. The developed facies were Gcm, Gp, Sm, Ss, Sh, Sl, St, Fl, Fsm, and C. The Gcm and Gp facies developed on conglomerate and gravelly sandstone lithologies. The Gcm facies were interpreted to have been deposited in a high-energy debris flow rich in clastics with a massive structure, and the thickness of these facies was 10 cm – 1 m (Figure 3b and d). The Gp facies were interpreted as the result of a migrating channel-filling process with a criss-cross structure and a facies thickness of 10 cm – 30 cm (Figure 3a). The Sm, Ss, Sh, Sl, and St facies developed in fine sandstone – gravel. The Sm facies had a massive structure, and the thickness of these facies was 45-51 cm.

The Sl facies had a cross-bedding structure with an angle of  $<15^\circ$ ; the facies thickness was 15-76 cm (Figure 3e). The Ss facies had a scour structure, which indicated channel filling. Often, there were rock lenses underneath it, and the thickness of these facies in sandstone deposits was 20 cm (Figure 3a). The Sh facies had a parallel bedding structure; generally, these layers were parallel to the current direction. The thickness of these facies in sandstone deposits was 30 cm. The Sl facies had a through cross bedding structure with a facies thickness of 11 cm. The Fl and Fsm facies developed in fine sandstone – silt. The Fsm facies had a massive structure, and the thickness of these facies was 93 cm. The Fl and Fsm facies developed in fine sandstone – silt. It was interpreted that these facies were leftover river deposits or backwater swamps, and usually, these layers represented waterlogged deposits during abandoned low-stage channels (Figure 3f). Facies C comprised black mudstone and coal lithology with a massive mud crack structure. The thickness of this layer reached 0.2 meters. These facies dominantly developed in the middle and lower parts of the succession in the study area. Facies C was interpreted as the result of overbank or abandoned channel deposits (Figure 3g).

### *Quartz-sandstone deposit*

Eight lithofacies were found in the Batupsair-gravel deposits based on the division of lithofacies [13]. The developed facies were Gmg, Sl, Ss, Sh, Sm, St, and Fsm. These deposits were not exposed locally and were directly adjacent to conglomerate deposits. The Gmg facies developed in the lower conglomerate lithology. These facies consisted of coarse-grained gravel and coarse-grained sandstone. The overlying deposits consisted of coarse, medium, and fine-grained sandstone. The Gmg conglomerate needed to be better sorted, matrix-supported, and exhibit fragmentary imbrication. The absence of sedimentary structures and the poor sorting and mixing of fine and coarse material suggested that the Gmg conglomerate was deposited by gravity flow and debris flow.

Facies Sl, Ss, Sh, Sm, and St were the dominant facies in this deposit, and sedimentary structures were found in the form of cross-bedding with an angle of  $<15^\circ$ , scour, massive, ripple lamination, and graded bedding. Low-energy traction currents deposited the Sh sandstone facies. Scour, massive, ripple-laminated structures showed changes in velocity and sediment load. The Fsm facies developed in siltstone lithology at the top of sandstone deposits with a massive structure. The Fsm facies most likely represented abandoned channel filling, as indicated by the presence of erosion surfaces or medium to coarse-grained sandstone.

**Table 2.** Architectural elements found in each deposits

<b>Architectural element</b>	<b>Conglomerate deposit</b>	<b>Sandstone-gravel deposit</b>
GB	v	-
SG	v	v
SB	v	v
CH	v	v
HO	v	-
FF	-	v



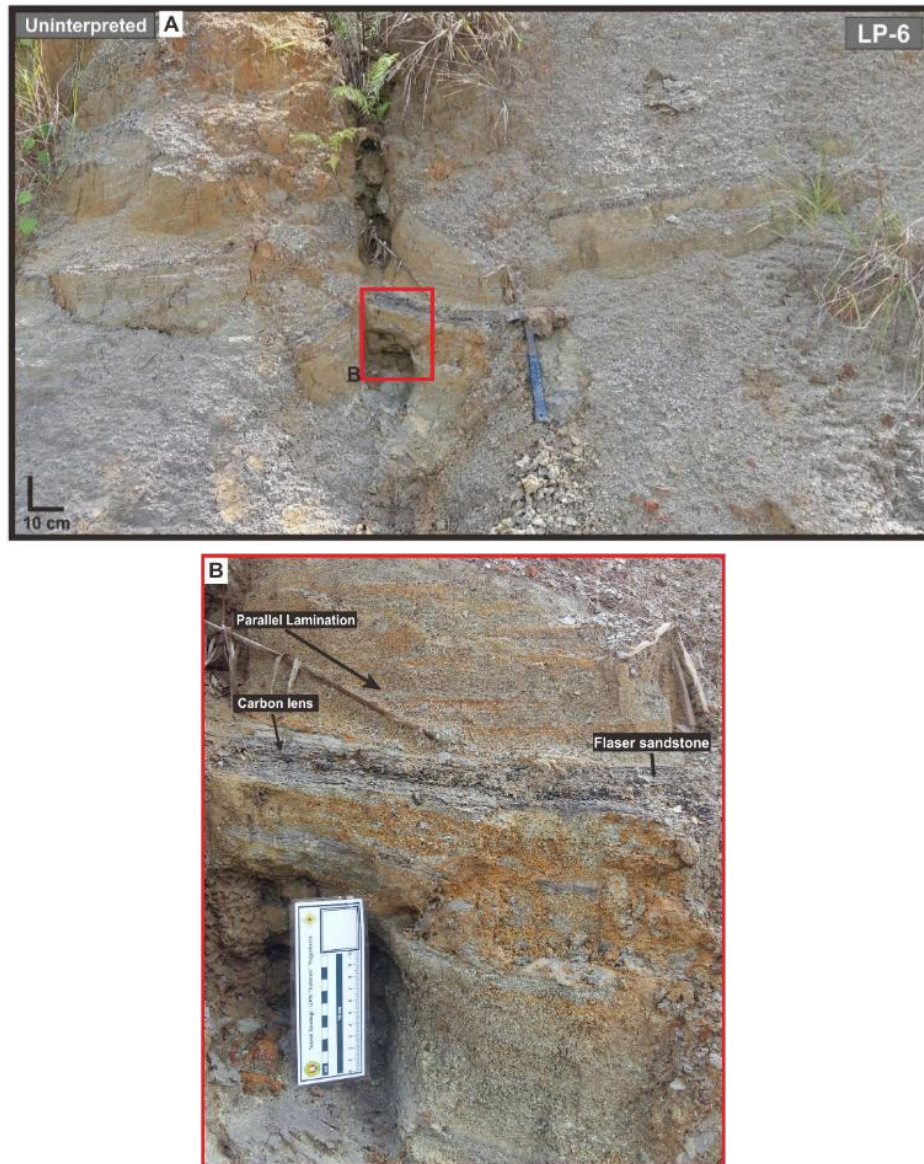


**Figure 4.** (a) Siltstone-tuff outcrop has a layered structure. (b) Close-up outcrop of siltstone-tuff interbedded laminated sandstone (facies Sh) with siltstone (facies FI and Fsm), and there are coal inserts (facies C).

### 3.3. Analysis of sedimentary architectural element

Six architectural elements [14] were channel (CH), scour hollows (HO), gravel bedform (GB), sediment gravity flows (SG), sandy bedform (SB), and floodplain fines (FF). Only some architectural elements were observed in every outcrop (see Table 2). These elements, defined by geometry and bounding surfaces [15], formed the basis for interpreting depositional environments.

#### *Conglomerate deposit*

##### *Sediment Gravity Flows (SG)*

Based on the results of facies analysis in gravelly sandstone deposits, facies Gp, Gcm, Gmg, Gh, Sm, Ss, and St were found. SG elements were narrow in shape, forming elongated lobes. This type was associated with GB and SB elements. Grading and inverse grading often appear; crisscrossed gravel at low angles indicates moving from debris flow to the traction system transport mechanism.

##### *Channel (CH)*

The facies Gmg, Sp, Sl, and Ss were found in this element. The channel element combined several architectural elements, showing a smooth upward pattern and a scouring or scouring at the base.



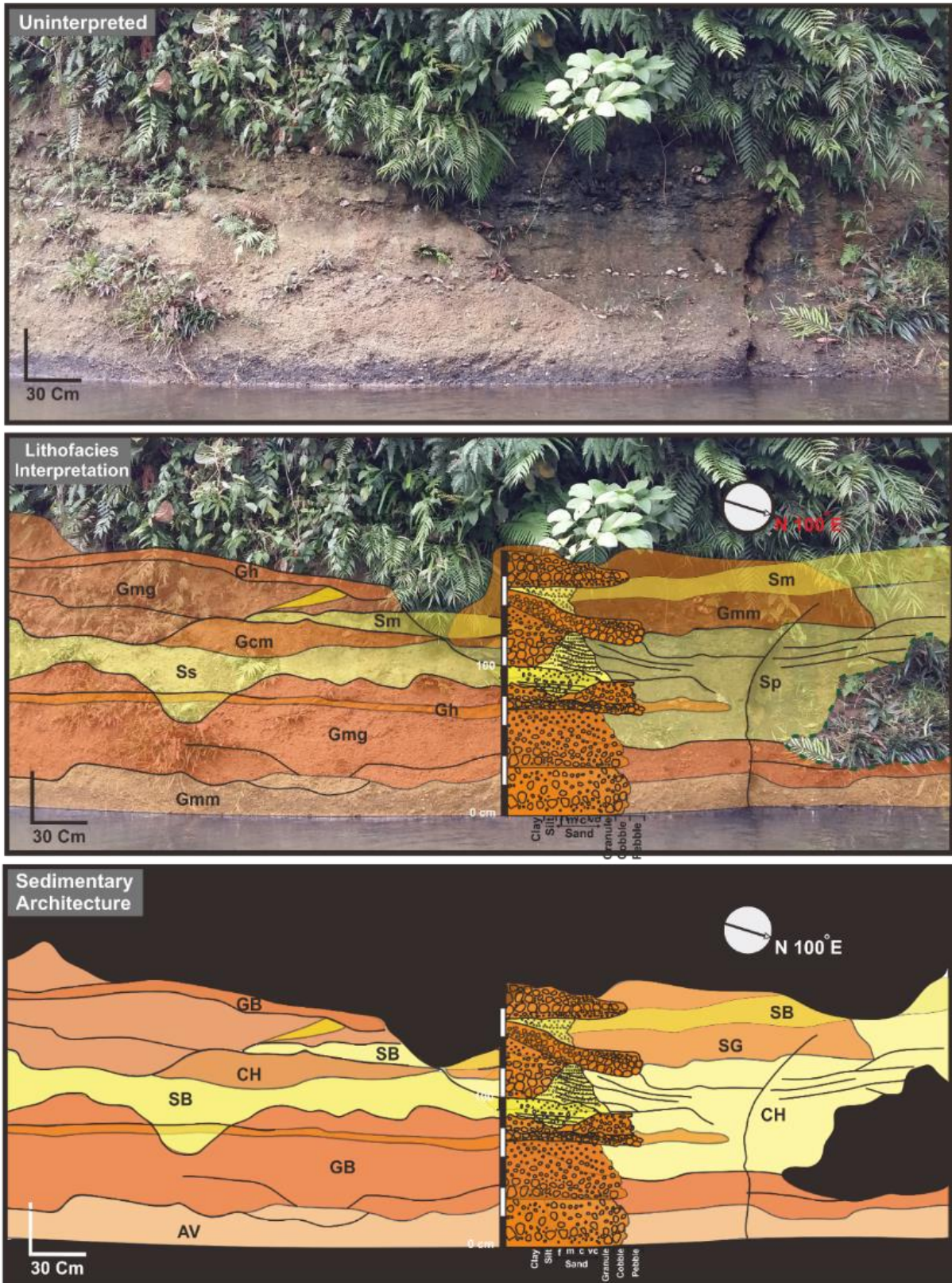


**Figure 5.** Interpretation of architectural element in conglomerate deposit of the ancient current direction facing east (a) Siltstone-tuff outcrop with a layered structure. (b) Close-up outcrop of siltstone-tuff interbedded laminated sandstone (facies Sh) with siltstone (facies FI and Fsm), and there are coal inserts (facies C).



#### *Scour Hollows (HO)*

In this element, the facies Gt, Gmg, Sl, and Ss were found in HO architectural elements in conglomerate deposits. The HO element resembled a small channel with a depth of 20 m and a width of around 250 m, with a bend-shaped bottom boundary concave upwards. It was a channel with a spade shape.

#### *Sandy bedform (SB)*

The facies Gcm, Sr, and Sm were found in this element. The architectural elements of Sandy Bedforms were usually layers of sandstone with a lens, layered, wedge geometry. The structures found in these facies were massive and scouring. The presence of the Gcm facies was interpreted to be deposited in high-energy debris flows rich in clastics.

#### *Gravel bedform (GB)*

The Gcm facies dominated the gravel bedform (GB) facies association. The GB facies association also comprised the Gp, Gh, Sm, and Sh facies. The dominated Gcm facies in this interval were interpreted to have been deposited by low-energy debris flows. The GB facies association was composed of sand-gravel grain-size material, which was deposited through a bedload mechanism. Therefore, this interval was interpreted as a dune element in the river flow. This suspicion was supported by a criss-cross structure, which indicates dune migration.

#### *Sandstone-gravel deposit*

##### *Channel (CH)*

The facies Gmg, Sp, Sl, and Ss were found in this element. The channel element combined several architectural elements, showing a smooth upward pattern and a scouring or grinding at the base. Another characteristic was that the shallower the channel depth, the wider the channel, and vice versa.

#### *Sandy bedform (SB)*

The facies St, Sm, Sr, and Sh were found in this element. The architectural elements of Sandy Bedforms were usually layers of sandstone with a lens, layered, wedge geometry. The structures found in these facies were massive, with ripple marks and wavy bedding.

#### *Gravel bedform (GB)*

The Gcm facies dominated the gravel bedform (GB) facies association. In addition, the GB facies association also consisted of the Gp and Sh facies. The thickness of the SB facies association reached 20 meters. The Gcm facies that dominated this interval were interpreted to have been deposited by low-energy debris flows. Looking at the GB facies association, composed of sand-gravel grain size material, this facies was deposited through a bedload mechanism. Therefore, this interval was an interpretation of a dune element in the river flow. This was supported by a criss-cross structure, which indicated dune migration.

#### *Floodplain (FF)*

Floodplain Fines (FF) architectural elements were part of the overbank deposits of the river body. This architectural element consisted of Fsm and C. The fine-grained facies was interpreted as a floodplain area. The finding of carbon streaks in wonderful sand and clay-sized lithology supported this suspicion. Flood plains were caused by the inability of the river body to withstand the flowing discharge.

#### *Quartz-sandstone deposit*

Based on the facies associations, five types of architectural elements were found in sandstone-quartz deposits (Figure 2) based on Miall classification [14], namely:

#### *Scour Hollows (HO)*

The HO element resembled a small channel, with a thickness in the profile of 6 m. This element was a spade-shaped channel composed of lithofacies Ss, Sl, Gmg, and Gt with sedimentary structures through cross-bedding, planar cross-bedding, scour, massive, and graded bedding.

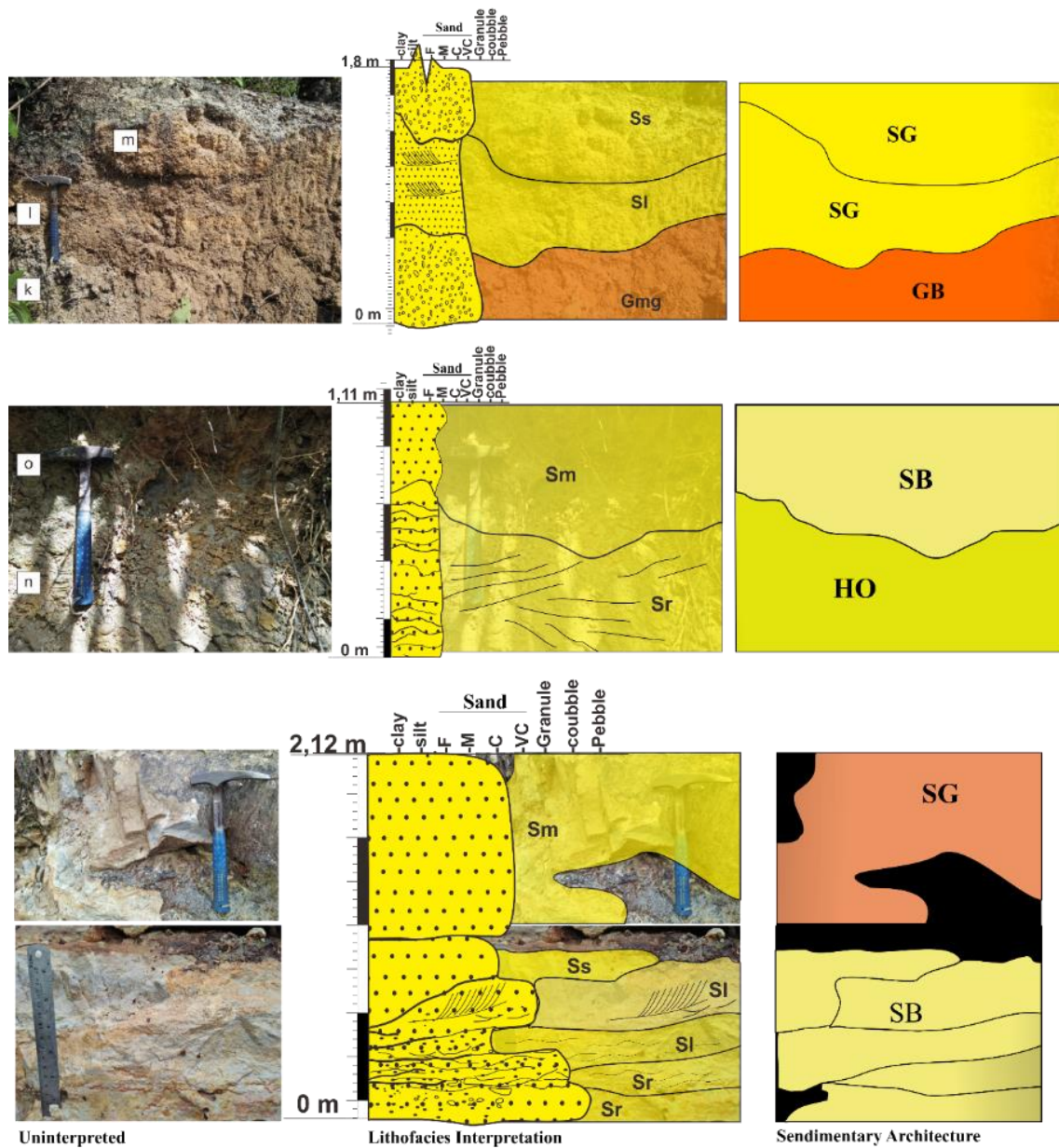


**Figure 6.** Interpretation of architectural element in Sandstone-Quartz deposit

*Channel (CH)*

The facies Gmg, Sr, Sl, and Ss were found in this element. In sandstone-quartz deposits, Channel elements were found (see Figure 5.1) at the bottom and top of the deposit. The Channel element combined several architectural elements, showing a smooth upward pattern and a scouring or grinding at the base.

*Sand bedform (SB)*

In this element, Sm, Sr, and Sh facies were found. In the Lemat sandstone-quartz unit, sand bedform elements were found (Figure 5.2) in the middle and upper parts of the unit.

*Floodplain (FF)*

In this element, the Fsm facies were found (Figure 5.8) as massive siltstones in the Lemat sandstone unit. This element characterized a deposition in left-behind rivers or back swamps.

*Lateral accretion (LA)*

In this element, Sr, Sm, and Ss facies were found as massive sandstone-quartz, quartz sandstone with a wavy layering structure in sandstone-quartz deposits.



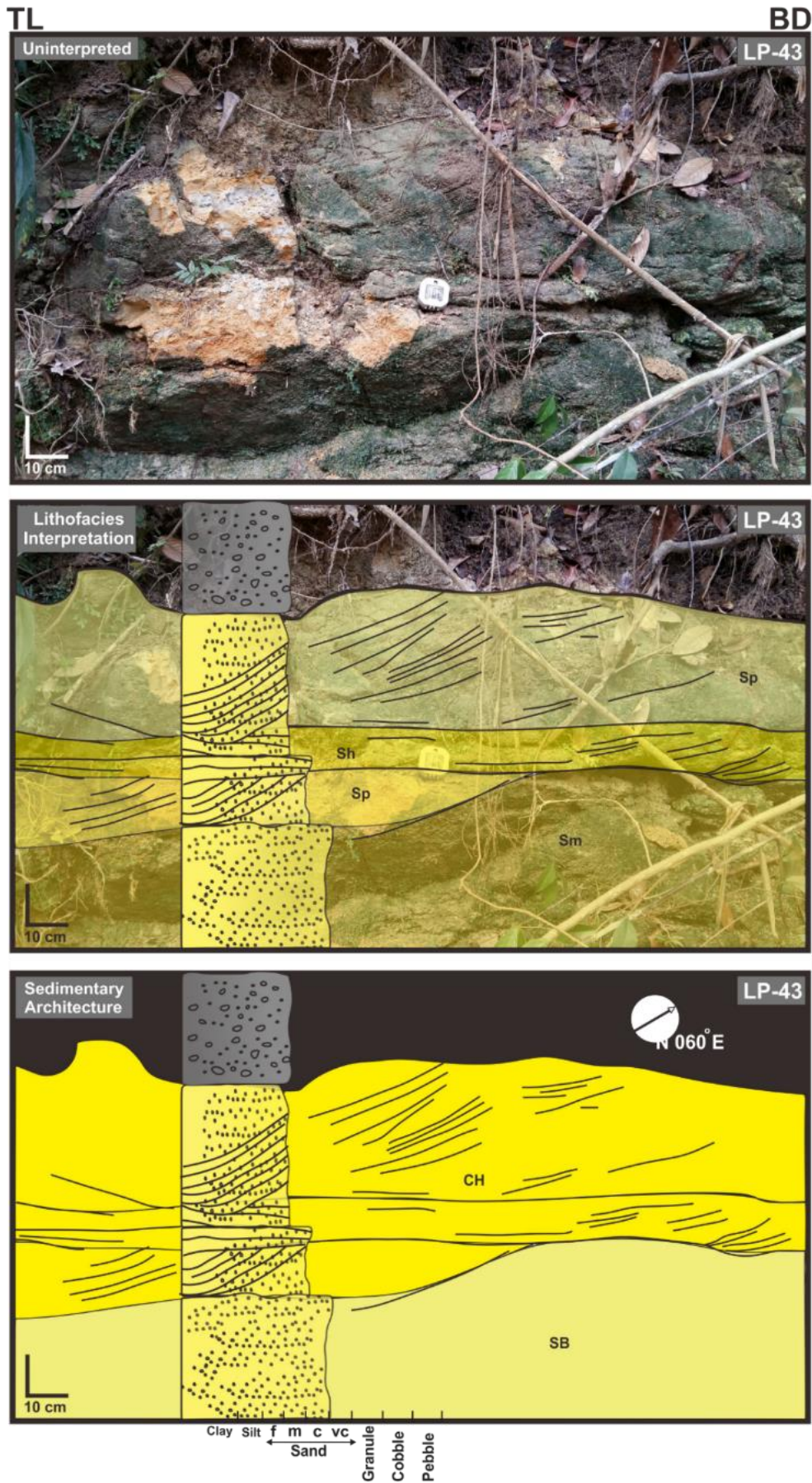


**Figure 7.** The first interpretation of architectural element in Sandstone-gravel deposit and ancient current face northeast



BL

TG

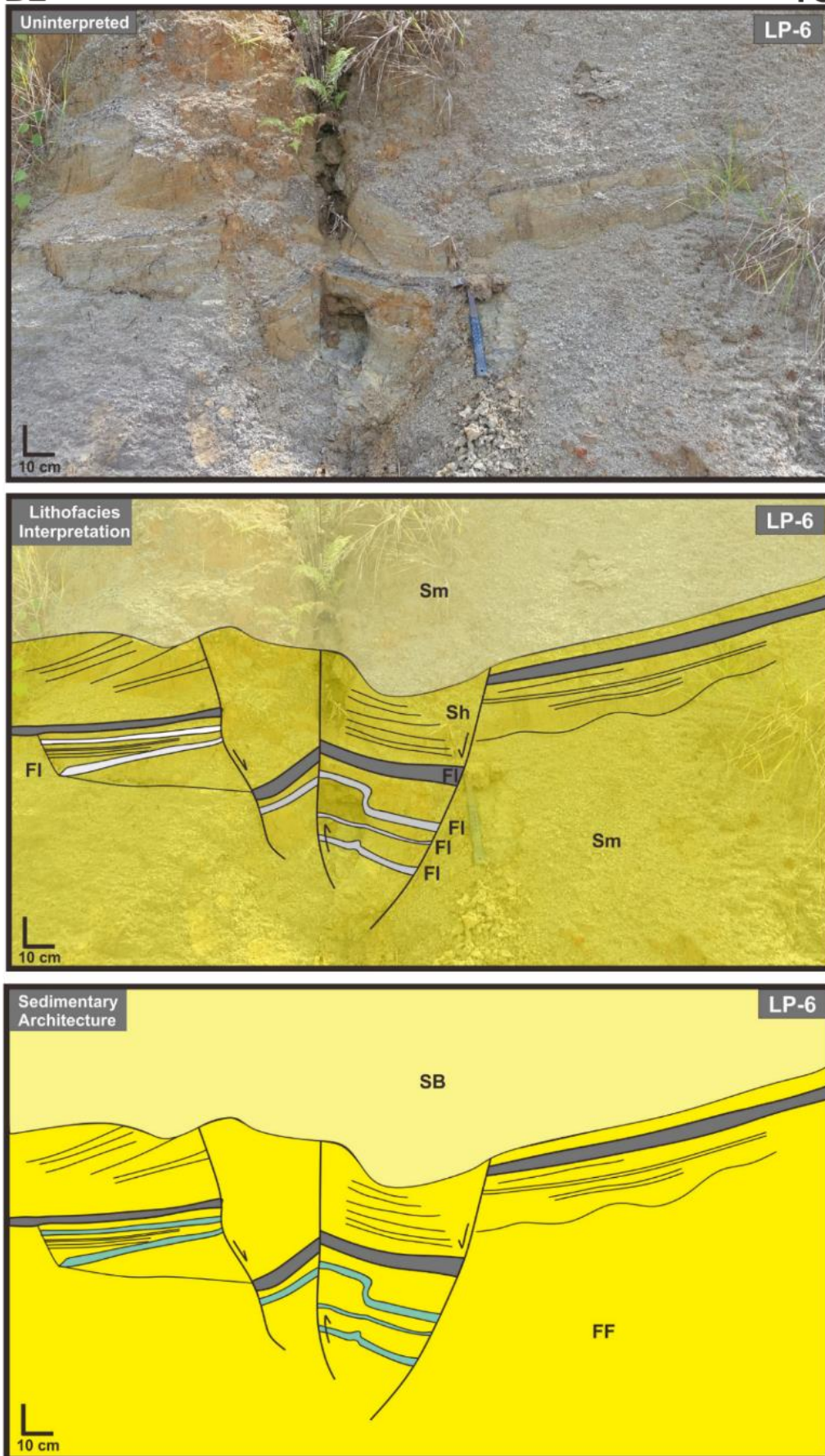
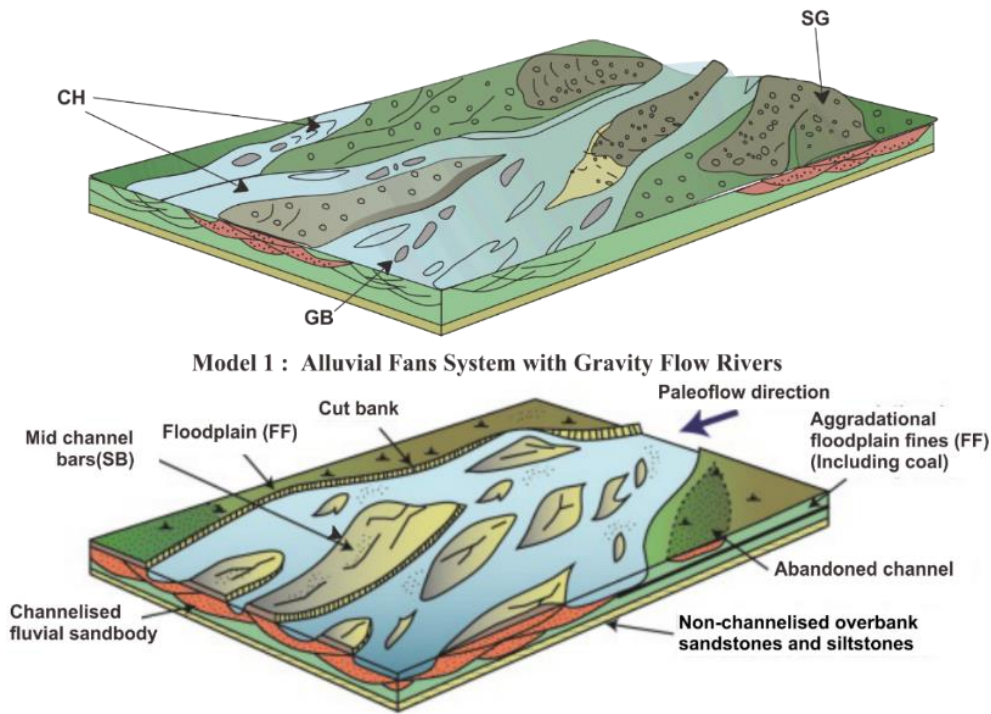


**Figure 8.** Second interpretation of architectural element in sandstone-gravel deposit





**Model 2 : Braided Rivers System with Shallow Channels and Gravel Bars**  
**Figure 9.** Deposit model of conglomerate deposit and sandstone-gravel in Lemat Formation

### 3.4. Depositional environment

In conglomerate deposits, architectural elements were found in the form of Sediment gravity flows (SG), sandy bedform (SB), gravel bedform (GB), channel (CH), scour hollows (HO), and floodplain fines (FF) (see Figure 5). This area's depositional environment is a braided channel system that cut and eroded itself. This is reflected in the energy dynamics and high flow velocity, resulting in material deposition with grain size (coarse-grained sandstone and conglomerate), interpreted as a channel-filling process. Then, in the following phase, fine sedimentary material appeared, interpreted as Floodplain fine deposits. The floodplain fines facies showed a current change from previously strong to weaker currents. Initially, the coarse grains settled at the bottom according to the existing rock mass, and then the refined grains settled at the very top because of the small density of the rock. This change in energy from high to low is likely caused by reduced sources of water supply and sediment material from upstream channels (Figure 5-7). In addition, the change in energy dynamics from high to low is likely attributed to reduced water and sediment supply from upstream channels [16].

The dominance of sedimentary material, which tends to be coarse, and the large number of facies associations GB, SG, and SB indicate many river bars. They are characteristic of braided rivers [14]. Braided rivers have a bed load sediment transport mechanism (creeping on the river bed). Braided river geometry, namely high slopes, wide river geometry, and the highest river slope among all types of rivers. It has straight to-curved river curves. Braided rivers have more than one channel (multi-channel). The two models obtained based on the results of the description [14] are the alluvial fans system with gravity flow river or gravel bed braided river and shallow, gravel-bed braided river (see Figures 7 and 8). The deposit model of conglomerate deposit and sandstone gravel in the Lemat Formation and the geological block diagram of conglomerate deposit and sandstone gravel can be seen in Figures 9 and 10. The first model in Figure 9 represents an alluvial fan system with gravity flow rivers, characterized by channels filled with sand and gravel and gravel forming gravel bars within these channels [16]. The second model depicts a braided river system with shallow channels and gravel bars, highlighting mid-channel sand bodies, floodplains, cut banks, abandoned channels, and non-channelized overbank deposits [16]. This model emphasizes the complex network of interweaving channels and the various sedimentary structures resulting from fluctuating water flow and sediment deposition.

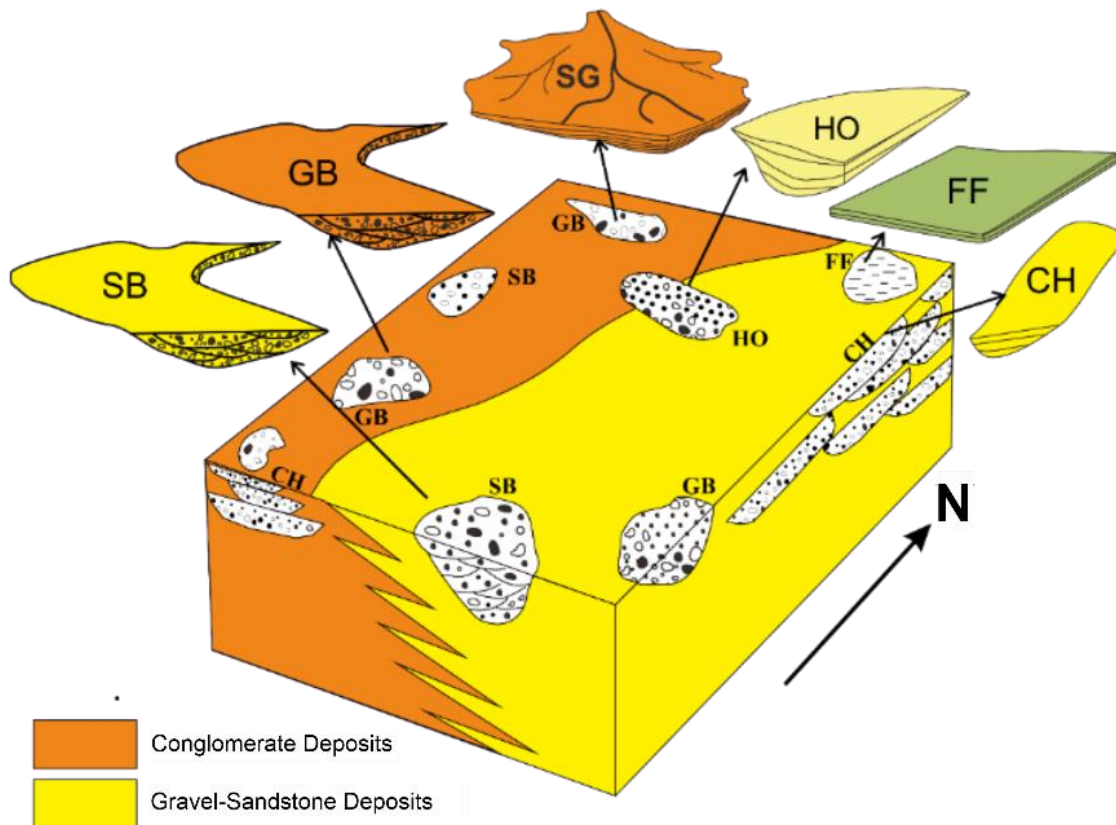


**Figure 10.** Geological block diagram of conglomerate deposit and sandstone-gravel

#### 4. Conclusion

Based on facies analysis, the stratigraphic succession in the study area shows a fluvial depositional environment in a braided river system. In this succession, facies are observed, which showed six architectural elements, namely GB (gravel bedform), SG (sediment gravity flow deposits), CH (channel), SB (sand bedforms), FF (floodplain fines), and scour hollows (HO). Based on an analysis of lithofacies and architectural elements in the research area, it was suggested that the research area was deposited in an environment with a braided river model with gravel braided rivers with sedimentary gravity flows.

#### Acknowledgment

We would like to express our sincere gratitude to the reviewers and the editorial team of the Journal of Earth and Marine Technology for their invaluable feedback and meticulous editing. Their insightful comments and suggestions significantly improved the quality of this manuscript.

#### References:

- [1] A. J. Barber, M. J. Crow, and J. S. Milsom, *Sumatra: Geology, Resources and Tectonic Evolution*. London: The Geological Society, 2005.
- [2] A. Pulunggono and N. R. Cameron, "Sumatran Microplates, their Characteristics and their Role in the Evolution of the Central and South Sumatra Basins," dalam *Proceeding 13th Annual Convention Indonesian Petroleum Association*, Jakarta, May, 1984.
- [3] S. Kasim and J. Armstrong, "Oil-oil correlation of the south sumatra basin reservoirs", *Journal of Petroleum and Gas Engineering*, vol. 6, no. 5, p. 54-61, 2015. <https://doi.org/10.5897/jpge2013.0162>
- [4] V. Napitupulu, M. Jannah, M. Silaen, & H. Darman, "Hydrocarbon columns of oil and gas fields in the south sumatra basin", *Berita Sedimentologi*, vol. 46, no. 1, p. 51-60, 2021. <https://doi.org/10.51835/bsed.2020.46.1.60>



- [5] M. G. Bishop, "South Sumatra Basin Province, Indonesia: The Lahat/Talang Akar Cenozoic Total Petroleum System," Colorado, U.S. Geological Survey, 2001, p. 22.
- [6] P. Putra and R. Raguwanti, "Hydrocarbon prospectivity and petroleum system in west Sumatra forearc basin", *Berita Sedimentologi*, vol. 46, no. 1, p. 44-50, 2021. <https://doi.org/10.51835/bsed.2020.46.1.59>
- [7] T. Koning, N. Cameron, & J. Clure, "Undiscovered potential in the basement exploring in Sumatra for oil and gas in naturally fractured and weathered basement reservoirs", *Berita Sedimentologi*, vol. 47, no. 2, p. 67-79, 2021. <https://doi.org/10.51835/bsed.2021.47.2.320>
- [8] F. Anggara, M. Riassetiawan, F. Assamarqandi, B. Sartika, I. Rizaldi, V. Syahraet al., "Screening criteria of underground coal gasification (ucg): a case study from mangunjaya area, south Sumatra basin, Indonesia", *IOP Conference Series: Earth and Environmental Science*, vol. 1071, no. 1, p. 012023, 2022. <https://doi.org/10.1088/1755-1315/1071/1/012023>
- [9] T. Koning, N. Cameron, & J. Clure, "Undiscovered potential in the basement exploring in Sumatra for oil and gas in naturally fractured and weathered basement reservoirs", *Berita Sedimentologi*, vol. 47, no. 2, p. 67-79, 2021. <https://doi.org/10.51835/bsed.2021.47.2.320>
- [10] R. Ryacudu, "Tinjauan Stratigrafi Paleogen Cekungan Sumatra Selatan," *Indonesian Association of Geologist: Sumatra Stratigraphy Workshop*, Bandung: Institut Teknologi Bandung, 2008, pp. 99-114.
- [11] Carrillat, A., Bora, D. S., Dubois, A., Kusdiantoro, F., Yudho, S., Wibowo, e. R. A., ... & Audemard, P. (2013). Integrated regional interpretation and new insight on petroleum system of south Sumatra basin, Indonesia. All Days. <https://doi.org/10.2118/165848-ms>
- [12] Yarmanto, et al., "Tertiary Tectonostratigraphy Development of Balam Depocenter, Central Sumatra basin Indonesia," dalam *Proceeding of the 5th Indonesian Petroleum Association Annual Convention*, pp. 35-45, 1995.
- [13] A. D. Miall, "Lithofacies Type and Vertical Profile Models in Braided River Deposits: a summary," dalam *Fluvial Sedimentology*, A. D. Miall, Ed., Canada Society Petroleum Geology Memoirs 5, 1978, pp. 597-604.
- [14] A. D. Miall, "Architectural-element analysis: a new method of facies analysis applied to fluvial deposits," *Earth Science Reviews*, vol. 22, pp. 261-308, 1985.
- [15] A. D. Miall, *The Geology of Fluvial Deposits: Sedimentary Facies, Basin Analysis and Petroleum Geology*, New York: Springer, 1996.
- [16] P. Lemenkova, "Analysis of the difference in depths and variation in slope steepness of the sunda trench, indonesia, east indian ocean", *Revista De Geomorfologie*, vol. 22, no. 1, p. 21-41, 2020. <https://doi.org/10.21094/rg.2020.096>